Equilibrium structure and energetics of CHNO isomers: Steps towards ab initio rovibrational spectra of quasi-linear molecules

M. Mladenovic, Marius Lewerenz

Chemical Physics **343**, 129-140 (2008)

Equilibrium structure and energetics of CHNO isomers: steps towards *ab initio* rovibrational spectra of quasi-linear molecules

Mirjana Mladenović* and Marius Lewerenz†
Laboratoire de Chimie Théorique, Bâtiment Lavoisier, Université Paris Est, Marne la Vallée, 5 boulevard Descartes, Champs sur Marne, 77454 Marne la Vallée Cedex 2, France

We report large-scale electronic structure calculations for fulminic acid, HCNO, isocyanic acid, HNCO, and cyanic acid, HOCN, in their ground electronic states. The coupled cluster CCSD(T) method including all single and double excitations and a perturbative term for connected triple substitutions is used in conjunction with large correlation consistent polarized valence basis sets of the form cc-pVXZ (X=2-6) and cc-pCVXZ (X=2-5). Our results show the importance of including all electrons in the correlation treatment to obtain a converged molecular structure for the extremely floppy HCNO molecule and the correct energetics of the three isomers. All electron correlation calculations and frozen core calculations with very large basis sets clearly converge towards a linear electronic minimum for HCNO surrounded by a very large flat region of the potential energy surface for hydrogen bending motions. For each of the three isomers we have computed the barrier to linearity along the respective minimum energy path and several spectroscopic parameters and equilibrium rotational constants.

Keywords: Ab initio calculation; CHNO; Equilibrium structure; Quasi-linear molecules; Potential energy surface

I. INTRODUCTION

Molecules with a non-linear electronic minimum but a low barrier to linearity allowing a large amplitude bending motion may exhibit rovibrational spectra with level patterns reminiscent of molecules with a rigid linear skeleton and are usually referred to as quasi-linear molecules.[1–3] The large amplitude bend contributes a vibrational angular momentum which couples with the overall rotational angular momentum. Furthermore the bending motion is frequently coupled with the high-frequency stretch modes. The combination of these features leads to particularly complicated rovibrational spectra, exhibiting many fascinating features, such as Fermi and l-type resonances, Coriolis coupling, and large centrifugal distortion.

Fulminic acid, HCNO, is one of the most important representatives of this class of molecules and has been subjected to extensive previous experimental[2,4–9] and theoretical[10–16] analyses. Winnewisser and Winnewisser[4] were the first to propose in 1971 a quasi-linear molecular model for the fulminic acid molecule. An unreasonably short r_s(HC) distance of 1.0266 Å was initially derived from the microwave data within a linear molecule model for HCNO.[4] A deviation from Bernstein's rule[17] for CH stretching fundamentals motivated Winnewisser et al. to suggest a non-linear equilibrium structure, possessing an HCN angle of ca. 162°. The classification of quasi-linear molecules proposed in Ref. 6 places HCNO rather close to the linear molecule limit. A semirigid bender study of Bunker et al.[10] led to the conclusion that HCNO has a linear equilibrium structure and bent vibrationally averaged structures. A small barrier to linearity of 11.5 cm^{-1} was determined for the effective ground-state potential energy profile along the HCN angle. Such a structure was actually called quasi-bent in Ref. 10.

The electronic structure problem of HCNO has turned out to be particularly hard, leading to strongly basis set and correlation method dependent results, such that the equilibrium geometry and the size of the barrier to linearity, if there is any, are still unclear. Whereas MP2, MP4, and MCSCF calculations favour a nonlinear structure, a linear equilibrium was found at the SCF, MP3, CISD, and CCSD levels of theory,[11,14] and also with CCSD(T)/TZ2P.[12] Koput et al.[14] deduced a small barrier to linearity of 7 cm^{-1} by means of CCSD(T)/cc-pVQZ. Several *ab initio* studies have additionally reported harmonic vibrational frequencies and/or energetics for the system [H,C,N,O].[13,15,16,18] So far, there is, however, only a single study providing variational results for rovibrational states of HCNO. In that study, Pinnavaia et al.[13] developed and employed a six-dimensional MP2/DZP potential enery surface, on which the optimized bent HCNO configuration is ca. 330 cm^{-1} more stable than the optimized linear configuration.

High-quality rovibrational calculations are the ultimate means to clarify the characteristic rovibrational spectral patterns by theoretical means. The starting point for such calculations is an accurate potential energy surface (PES), which samples large portions of the available configuration space, covering at least those degrees of freedom which are essential for understanding the internal molecular dynamics. The quasi-linear species

HXYZ with a hydrogen atom attached to a (nearly linear) chain of heavy atoms pose a very demanding computational task from both the electronic structure and rovibrational point of view because of the strongly anharmonic large amplitude HXY bending vibration.

With the ultimate goal to develop a full-dimensional potential energy surface for the fulminic acid molecule in its electronic ground state, our initial purpose was to study the equilibrium structure with a high level of accuracy and to identify the best trade-off between accuracy and expense of computer time. However, our calculations beyond the frozen-core approximation showed a prominent contribution of core correlation at the equilibrium internuclear geometry of HCNO. Since this quantity is relevant for the calculation of energetics of the [H,C,N,O] system, we have extended our work to include HNCO and HOCN, too.

Isocyanic acid, HNCO, is the most stable among all CHNO isomers.[19] It is energetically followed by cyanic acid, HOCN, and fulminic acid, HCNO. From the historical point of view, the isomers are important because of the first experimental evidence of isomerism in 1826, when Liebig and Wöhler agreed that HNCO and HCNO possess the same chemical composition, but are structurally distinct.[20] The CHNO isomers (most prominently HNCO) are expected to participate in interstellar chemistry and to play a major role in the RAPRENO$_x$ process for NO reduction in combustion.[18,21–23] HNCO is considered also to be quasi-linear, exhibiting a barrier to linearity of 1899 cm^{-1} according to a semirigid bender analysis of Niedenhoff et al.[24] Whereas both HCNO and HNCO possess very rich rovibrational spectra in the gas phase,[2,4–9] HOCN could be studied solely under matrix conditions.[20,25] For HNCO and HOCN, Pinnavaia et al. reported only perturbational results.[13] We refer to Refs.13,14,16 for an overview of the previous experimental and theoretical work on the CHNO isomers.

Energy levels associated with a large amplitude bending vibration may develop a pattern typical for linear molecules, even for a bent equilibrium structure.[1,26] This was found in our recent study[27] on cyanocarbene, HCCN. In spite of a nonlinear equilibrium structure, characterized by $\angle(\mathrm{HCC})_e$ of 147° and $\angle(\mathrm{CCN})_e$ of 175° for a MR-ACPF PES, the rovibrational energy levels of the radical were easily assigned following the conventional linear molecule notation. This phenomenon hinges on the barrier to linearity, determined to be 287 cm^{-1} for HCCN. Numerically exact rovibrational states of HCCN were calculated for $J = 0-4$, using the method described in Ref. 28. This type of treatment is the next logical step of our HCNO project.

In the present work, extensive *ab initio* calculations of the electronic ground state with coupled cluster techniques and large basis sets have been performed for each of the three isomers studied. Two families of basis sets were employed to approach the one-particle basis-set limit, including valence and all-electron correlation (Section II). The geometries of the minima have been optimized via numerical gradient techniques (Section III A). The barriers to linearity and isomerization energies have been derived (Section III B). The harmonic vibrational frequencies have been computed in order to characterize the stationary points (Section III C). The minimum energy paths along the bending angle HXY have been obtained for planar HCNO, HNCO, and HOCN by relaxing the other coordinates (Section III C).

II. ELECTRONIC STRUCTURE CALCULATIONS

The *ab initio* calculations presented below have been carried out by means of the coupled-cluster method, which explicitly includes all single and double excitations, as well as an noniterative perturbative treatment of connected triple substitutions. Dunning's correlation consistent double (X=2), triple (X=3), quadruple (X=Q), quintuple (X=5), and sextuple (X=6) polarized valence basis sets, commonly termed cc-pVXZ, have been used.[29]

Initially only valence electrons were correlated (the frozen-core approximation). Our test calculations for all-electron correlation, however, quickly showed that inclusion of the three 1s-like core orbitals located on carbon, nitrogen, and oxygen into the active space has an important influence on the geometrical parameters of HCNO. We have, thus, decided to study in detail also the correlation consistent polarized core-valence basis sets, usually called cc-pCVXZ, employing X=2-5. The cc-pCVXZ basis set family was developed by Woon and Dunning,[30] by augmenting the original cc-pVXZ sets with supplementary functions especially designed for core-core and core-valence correlations. In the case of cc-pCV5Z, representing the highest quality cc-pCVXZ basis set employed in the current work, the standard cc-pV5Z set is extended by adding $(4s, 4p, 3d, 2f, 1g)$, leading to $(18s, 12p, 7d, 5f, 3g, 1h) \rightarrow [10s, 9p, 7d, 5f, 3g, 1h]$ for carbon, nitrogen, and oxygen, whereas we have $(8s, 4p, 3d, 2f, 1g) \rightarrow [5s, 4p, 3d, 2f, 1g]$ for hydrogen. For [H,C,N,O], the basis sets cc-pV5Z and cc-pCV5Z contain 328 and 490 contracted Gaussian-type orbitals, respectively.

Full geometry optimizations were performed for each of the basis sets employed. To characterize the nature of the stationary points, Hessian matrices were computed and diagonalized. All calculations were performed with the MOLPRO quantum chemistry program package,[31] with the implementations of the CCSD method due to Hampel et al.[32] and of the perturbative triple corrections due to Deegan and Knowles[33]. Numerical derivatives were used in the geometry optimization and harmonic vibrational frequency computations, following the procedure of Eckert et al.[34] and of Rauhut et al.,[35] respectively.

The coordinate space was parametrized in terms of bond-distance-bond-angle coordinates, described by three bond lengths, r(HX), r(XY), and r(YZ), two in-plane bending angles, $\angle$(HXY) and $\angle$(XYZ), and one

dihedral angle for a HXYZ molecule.

III. RESULTS

HCNO, HNCO, and HOCN belong to the class of molecules with sixteen valence electrons, which includes e.g. CO_2 and HN_3.[36] Previous studies indicated that the three isomers studied here possess planar equilibrium structures of *trans* type.[13] In C_s symmetry, the reference (SCF) electronic configuration is given by (*same*) $(1a'')^2(8a')^2(2a'')^2(9a')^2$ for HCNO and by (*same*) $(1a'')^2(8a')^2(9a')^2(2a'')^2$ for HNCO and HOCN, where the common contribution (*same*) reads $(1a')^2(2a')^2(3a')^2(4a')^2(5a')^2(6a')^2(7a')^2$. In the A' ground electronic state, the highest occupied orbital of HNCO and HOCN is thus the nonbonding out-of-plane $2a''$ orbital. One may note that the orbitals $(8a', 1a'')$ and $(9a', 2a'')$ of HCNO at the nonlinear CCSD(T) equilibrium geometry (see Tab. I) have nearly degenerate RHF/cc-pV5Z energies of respectively $(-0.6786E_h, -0.6798E_h)$ and $(-0.4094E_h, -0.4096E_h)$, resembling a linear molecule situation (π orbitals).

The RHF/cc-pV5Z dipole moment vector for the CCSD(T)/cc-pV5Z equilibrium structures has magnitudes of 4.225 D, 2.245 D, and 4.053 D for HCNO, HNCO, and HOCN, respectively and magnitudes of 4.290 D, 3.260 D, and 2.164 D at the lowest energy linear geometries. The components ($\mid \mu_a \mid, \mid \mu_b \mid$) of the dipole moment vector are (0.234 D, 4.218 D) for HCNO, (1.569 D, 1.619 D) for HNCO, and (1.642 D, 3.715 D) for HOCN.

The quality of coupled cluster results with respect to a single reference electron correlation procedure may be assessed by means of the T_1 diagnostic,[37] which gives the norm of the t_1 amplitude. It is believed that CCSD may cope with nondynamical correlation up to a T_1 diagnostic of 0.02, as recommended in Refs. 37,38. In the case of the CHNO isomers, the highest T_1 diagnostic value of ca. 0.02 is found for cc-pVXZ with only valence correlation, dropping to ca. 0.018 in the case of all-electron correlation. Beyond the frozen core approximation, we obtained T_1 of ca. 0.016 and 0.013 for HNCO and HOCN, respectively. Our result for HNCO is compatible with the finding of East et al.[18] who reported the T_1 diagnostic for the valence correlation case, and concluded that the multireference character is not very high in HNCO.

In the following text, (all) following a basis set identification indicates that all electrons are included in the correlation treatment.

A. Equilibrium structures

Tables I, II, and III contain the geometrical parameters for planar and linear conformations of HCNO, HNCO, and HOCN, respectively. The geometries were optimized at the CCSD(T) level of theory employing two families of basis sets, cc-pVXZ and cc-pCVXZ. Valence and all electron correlations were evaluated. In Tables I, II, and III structural parameters obtained for the basis set of highest quality are highlighted by bold numbers. Equilibrium rotational constants A_e, B_e, C_e were determined and are collected in Table IV for selected basis sets. Table V provides an overview of the relative energies of the isomers. Our results for cc-pVDZ, cc-pVTZ, and cc-pVQZ basis sets displayed in Table I for HCNO agree perfectly with the values previously reported by Koput et al.[14] The equilibrium CCSD(T)/cc-pVQZ geometry obtained for HOCN by Schuurman et al.[16] differs however in r_e(CN)=2.1923 a_0 by 0.0025 a_0 from our value r_e(CN)=2.1948 a_0 reported in Table III. On the other hand, our cc-pVXZ results for $X = 2-4$ and all electron correlation show excellent agreement with those obtained by Demaison et al.[39] for planar HNCO and the optimized geometries at cc-pVTZ level calculated in Refs. 40 and 41.

The results for HCNO constrained to planar geometries with the cc-pVXZ series of basis sets and valence correlation only (upper part of Table I), clearly show convergence to better than [0.0003 a_0, 0.0015 a_0, 0.0003 a_0, 2.2°, 0.5°] for [$r_e(HC)$, $r_e(CN)$, $r_e(NO)$, $\angle$(HCN)$_e$, $\angle$(CNO)$_e$] at the final cc-pV6Z level. For the cc-pVXZ series in the all-electron situation, the convergence of the cc-pV5Z(all) results is better than [0.0027 a_0, 0.0040 a_0, 0.0011 a_0, 0.8°, 0.2°], whereas we have [0.0007 a_0, 0.0036 a_0, 0.0013 a_0, 4.4°, 0.9°] for the cc-pCV5Z(all) values in the cc-pCVXZ(all) series. For HCNO constrained to linear arrangements (lower part of Table I), all three distances are converged within 0.0005 a_0, 0.0040 a_0, and 0.0020 a_0 for cc-pV6Z, cc-pV5Z(all), and cc-pCV5Z(all), respectively.

The data in Table I clearly indicate major difficulties to obtain a well converged minimum energy structure, at least in angular space. The HCN bending angle of planar HCNO shows variations up to 30° upon basis set improvement with a definite tendency towards linearity. One may also note an abrupt change in both the HCN and CNO angles in Fig. 1 in the cc-pVXZ(all) series. The best equilibrium HCN bending angles are 170.8°, 176.4°, and 173.1° (scatter of 5.6°) with cc-pV6Z, cc-pV5Z(all), and cc-pCV5Z(all) basis sets, and equilibrium CNO angles of 177.9°, 179.2°, and 178.4° (scatter of 1.4°), respectively. Inspection of the lower part of Table I with results for linear HCNO reveals that the HCNO molecule is in reality linear at the CCSD(T)/cc-pV6Z, CCSD(T)/cc-pV5Z(all), and CCSD(T)/cc-pCV5Z(all) levels of theory, the linear form being more stable by a fraction of a cm^{-1}. The failure of the unconstrained optimization to reach this structure indicates a large and exceedingly flat region of the potential energy surface with energy changes near the numerical accuracy limit of standard total energy calculations. One may note that the optimized planar and linear HCNO conformations possess very similar bond lengths. The convergence to the linear arrangement as the electronic minimum is clearly bet-

TABLE I: Total energies E_{min} and E_{lin} at optimized planar and linear configurations, bond lengths (in a_0), and bond angles (in degrees) for fulminic acid, HCNO, obtained at the CCSD(T) level of theory for cc-pVXZ (X=2-6) and cc-pCVXZ (X=2-5) basis sets. The height of the barrier to linearity is calculated as E_{bar}=E_{lin}-E_{min}. All electron results for the basis sets cc-pVXZ and cc-pCVXZ are denoted by cc-pVXZ(all) and cc-pCVXZ(all), respectively.

planar HCNO	r_e(HC)	r_e(CN)	r_e(NO)	$\angle$(HCN)$_e$	$\angle$(CNO)$_e$	E_{min} /E_h
cc-pVDZ	2.0433	2.2601	2.2750	146.24	171.96	-168.158163
cc-pVTZ	2.0085	2.2152	2.2722	157.61	174.83	-168.321390
cc-pVQZ	2.0059	2.2012	2.2724	165.14	176.58	-168.372212
cc-pV5Z	2.0051	2.1971	2.2742	168.65	177.35	-168.388547
cc-pV6Z	**2.0048**	**2.1956**	**2.2745**	**170.84**	**177.88**	**-168.394263**
cc-pVDZ(all)	2.0415	2.2581	2.2736	146.71	172.11	-168.164556
cc-pVTZ(all)	1.9981	2.2074	2.2636	158.97	175.39	-168.365137
cc-pVQZ(all)	1.9998	2.1918	2.2690	175.64	179.02	-168.463134
cc-pV5Z(all)	**1.9971**	**2.1878**	**2.2701**	**176.45**	**179.23**	**-168.498786**
cc-pCVDZ(all)	2.0398	2.2548	2.2736	147.00	172.21	-168.278027
cc-pCVTZ(all)	2.0069	2.2077	2.2636	159.98	175.43	-168.484504
cc-pCVQZ(all)	2.0030	2.1945	2.2693	168.76	177.44	-168.546525
cc-pCV5Z(all)	**2.0023**	**2.1909**	**2.2706**	**173.13**	**178.36**	**-168.565759**
linear HCNO	r_e(HC)	r_e(CN)	r_e(NO)	E_{lin} /E_h	E_{bar} /cm^{-1}	
cc-pVDZ	2.0318	2.2326	2.2855	-168.156973	261.34	
cc-pVTZ	2.0042	2.2034	2.2777	-168.321197	42.38	
cc-pVQZ	2.0041	2.1959	2.2750	-168.372179	7.44	
cc-pV5Z	2.0041	2.1940	2.2757	-168.388542	0.81	
cc-pV6Z	**2.0042**	**2.1935**	**2.2757**	**-168.394264**	**-0.33**	
cc-pVDZ(all)	2.0304	2.2315	2.2839	-168.163439	245.13	
cc-pVTZ(all)	1.9950	2.1976	2.2684	-168.364961	38.68	
cc-pVQZ(all)	1.9997	2.1914	2.2692	-168.463134	-0.03	
cc-pV5Z(all)	**1.9969**	**2.1875**	**2.2702**	**-168.498788**	**-0.44**	
cc-pCVDZ(all)	2.0287	2.2286	2.2832	-168.276957	234.42	
cc-pCVTZ(all)	2.0036	2.1983	2.2727	-168.484389	23.44	
cc-pCVQZ(all)	2.0019	2.1916	2.2708	-168.546515	2.19	
cc-pCV5Z(all)	**2.0017**	**2.1896**	**2.2713**	**-168.565763**	**-0.87**	

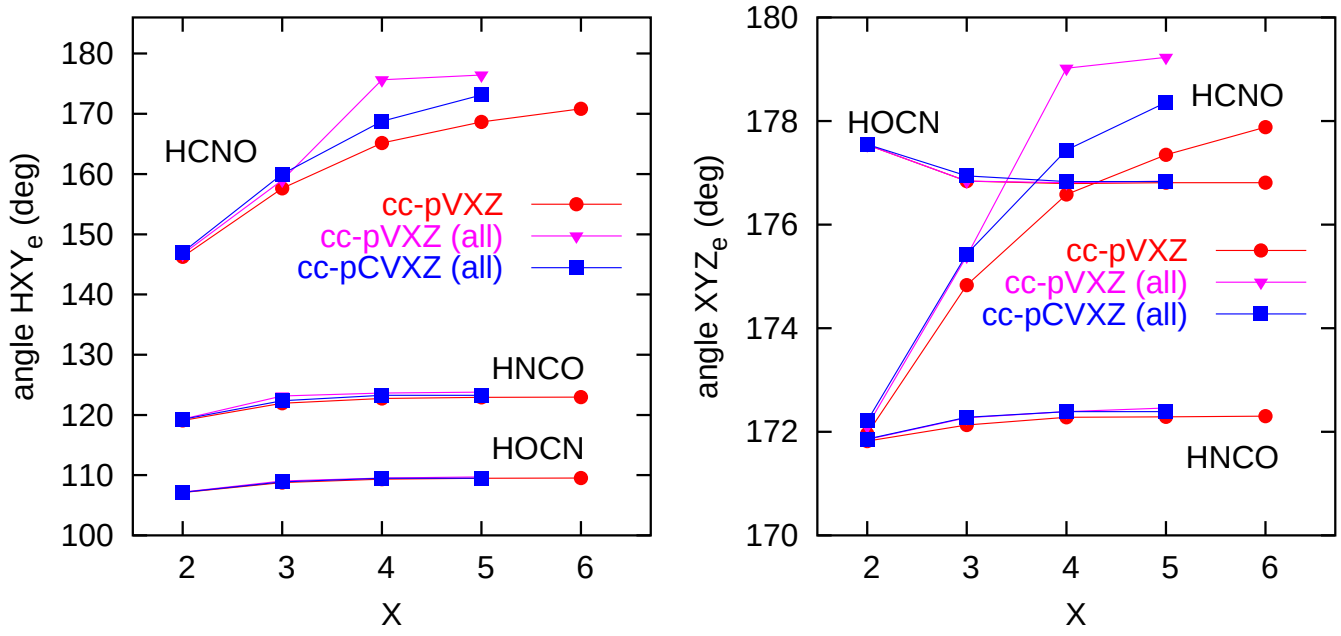

FIG. 1: Variation of the equilibrium HXY and XYZ angles with the cardinal number X of the cc-pVXZ, cc-pVXZ(all), and cc-pCVXZ(all) basis sets for planar HCNO, HNCO, and HOCN.

TABLE II: Optimized structural parameters of isocyanic acid, HNCO. For more details, see Table I.

planar HNCO	r_e(HN)	r_e(NC)	r_e(CO)	$\angle$(HNC)$_e$	$\angle$(NCO)$_e$	E$_{min}$ /E_h
cc-pVDZ	1.9240	2.3376	2.2266	119.10	171.82	-168.268465
cc-pVTZ	1.9004	2.3083	2.2106	121.95	172.13	-168.432782
cc-pVQZ	1.8982	2.3015	2.2040	122.72	172.28	-168.484107
cc-pV5Z	1.8983	2.3004	2.2029	122.91	172.29	-168.500436
cc-pV6Z	**1.8984**	**2.2999**	**2.2025**	**122.96**	**172.30**	**-168.506138**
cc-pVDZ(all)	1.9224	2.3357	2.2257	119.29	171.85	-168.274865
cc-pVTZ(all)	1.8948	2.2987	2.2051	123.14	172.27	-168.475476
cc-pVQZ(all)	1.8932	2.2942	2.1997	123.62	172.39	-168.574631
cc-pV5Z(all)	**1.8934**	**2.2914**	**2.1969**	**123.78**	**172.46**	**-168.610519**
cc-pCVDZ(all)	1.9218	2.3336	2.2238	119.27	171.86	-168.388591
cc-pCVTZ(all)	1.8978	2.3023	2.2059	122.37	172.28	-168.595999
cc-pCVQZ(all)	1.8958	2.2955	2.2000	123.27	172.39	-168.658308
cc-pCV5Z(all)	**1.8956**	**2.2943**	**2.1988**	**123.50**	**172.40**	**-168.677463**
linear HNCO	r_e(HN)	r_e(NC)	r_e(CO)	E$_{lin}$ /E_h	E$_{bar}$ /cm^{-1}	
cc-pVDZ	1.8836	2.2587	2.2471	-168.257037	2508	
cc-pVTZ	1.8655	2.2347	2.2298	-168.423660	2002	
cc-pVQZ	1.8654	2.2302	2.2231	-168.475344	1923	
cc-pV5Z	1.8658	2.2295	2.2220	-168.491746	1907	
cc-pV6Z	**1.8659**	**2.2292**	**2.2216**	**-168.497487**	**1899**	
cc-pVDZ(all)	1.8824	2.2576	2.2460	-168.263635	2465	
cc-pVTZ(all)	1.8609	2.2287	2.2239	-168.467642	1721	
cc-pVQZ(all)	1.8617	2.2258	2.2181	-168.566668	1748	
cc-pV5Z(all)	**1.8622**	**2.2230**	**2.2155**	**-168.602508**	**1758**	
cc-pCVDZ(all)	1.8812	2.2549	2.2442	-168.377392	2458	
cc-pCVTZ(all)	1.8643	2.2302	2.2251	-168.587091	1952	
cc-pCVQZ(all)	1.8639	2.2262	2.2188	-168.649892	1847	
cc-pCV5Z(all)	**1.8641**	**2.2254**	**2.2176**	**-168.669183**	1817	

ter in the all electron calculations. A linear equilibrium structure is compatible with the results of Bunker et al.[10] who used the semirigid bender model to study the rovibrational spectra of HCNO and concluded that HCNO is likely linear with an equilibrium geometry of [r_e(HN), r_e(NC), r_e(CO)] equal to [2.0031 a_0, 2.2091 a_0, 2.2658 a_0]. These values exhibit, however, noticeable deviations (up to 0.02 a_0) from our results (Table I) for both linear and planar conformations.

The equilibrium heavy atom XYZ bending angle found in planar arrangement optimizations is larger than 170° for all three isomers, i.e. ca. 178° for HCNO, 177° for HOCN, and 172° for HNCO. A quick glance at Tables II and III reveals that the equilibrium bending angles of HNCO and HOCN are, unlike HCNO, very stable during the geometry optimization within each series of basis sets, showing only minor and monotonic changes. Going from triple to quintuple ζ basis set quality, the HXY and XYZ angles vary by at most 1° and 0.2°, respectively, and converge to very similar values (bold numbers). This is also evident from Fig. 1, which shows the equilibrium HXY and XYZ angles as functions of the basis set cardinal number X. Excellent and almost universally monotonic convergence within each series is observed for interatomic distances with, however, somewhat different final values.

Experimental determinations of the equilibrium structure of HOCN are not available due to the absence of gas phase observations. For HNCO East et al. derived[18] an empirical equilibrium structure of [r_e(HN), r_e(NC), r_e(CO), $\angle$(HNC)$_e$, $\angle$(NCO)$_e$] equal to [1.8954 a_0, 2.2953 a_0, 2.1985 a_0, 123.34°, 172.22°] from the known experimental rotational constants A_0, B_0, C_0 and theoretical rotation-vibration coupling constants (α_e). Among our HNCO results of Table II, the CCSD(T)/cc-pCV5Z(all) values show the best agreement within [0.0002 a_0, -0.0010 a_0, 0.0003 a_0, 0.16°, 0.18°] with the finding from Ref. 18. This is a very encouraging result because this should be the most consistent combination of basis set and correlation approach. The importance of the core correlation effect for the prediction of the HNCO angles was previously pointed out by Demaison et al.[39]

The variation of the absolute equilibrium energy of HCNO (Table I) with the basis set cardinal number X is graphically presented in Fig. 2. Only the planar case is shown, since energies of planar and linear HCNO appear identical on the scale of the figure. The absolute difference between the $X = 4$ and $X = 5$ results in Fig. 2 is ca. 0.016, 0.036, and 0.019 E_h for cc-pVXZ, cc-pVXZ(all), and cc-pCVXZ(all), respectively.

The equilibrium rotational constants calculated from the structural parameters of Tables I, II, and III are summarized in Table IV. For these evaluations, the atomic masses for ^{1}H, ^{12}C, ^{14}N, and ^{16}O are taken from Ref. 42. For each of the three CHNO isomers, the constants B_e,

TABLE III: Optimized structural parameters of cyanic acid, HOCN. For more details, see Table I.

planar HOCN	r_e(HO)	r_e(OC)	r_e(CN)	$\angle$(HOC)$_e$	$\angle$(OCN)$_e$	E$_{min}$ /E_h
cc-pVDZ	1.8371	2.4907	2.2294	107.12	177.54	-168.231416
cc-pVTZ	1.8247	2.4713	2.2016	108.76	176.84	-168.394918
cc-pVQZ	1.8213	2.4632	2.1948	109.34	176.79	-168.445427
cc-pV5Z	1.8213	2.4614	2.1935	109.49	176.81	-168.461521
cc-pV6Z	**1.8214**	**2.4607**	**2.1931**	**109.54**	**176.81**	**-168.467105**
cc-pVDZ(all)	1.8361	2.4887	2.2283	107.18	177.54	-168.237624
cc-pVTZ(all)	1.8217	2.4625	2.1947	109.02	176.84	-168.436786
cc-pVQZ(all)	1.8181	2.4563	2.1896	109.53	176.81	-168.535393
cc-pV5Z(all)	**1.8180**	**2.4542**	**2.1865**	**109.71**	**176.84**	**-168.571113**
cc-pCVDZ(all)	1.8358	2.4879	2.2255	107.16	177.55	-168.351416
cc-pCVTZ(all)	1.8226	2.4665	2.1954	108.88	176.94	-168.558021
cc-pCVQZ (all)	1.8199	2.4581	2.1898	109.49	176.83	-168.619465
cc-pCV5Z(all)	**1.8195**	**2.4561**	**2.1884**	**109.66**	**176.83**	**-168.638383**
linear HOCN	r_e(HO)	r_e(OC)	r_e(CN)	E$_{lin}$ /E_h	E$_{bar}$ /cm^{-1}	
cc-pVDZ	1.7910	2.3897	2.2366	-168.181592	10935	
cc-pVTZ	1.7821	2.3699	2.2081	-168.349713	9921	
cc-pVQZ	1.7807	2.3641	2.2016	-168.401664	9605	
cc-pV5Z	1.7814	2.3631	2.2003	-168.418284	9489	
cc-pV6Z	**1.7817**	**2.3627**	**2.1999**	**-168.424029**	**9453**	
cc-pVDZ(all)	1.7902	2.3883	2.2353	-168.187964	10901	
cc-pVTZ(all)	1.7784	2.3616	2.2008	-168.393175	9571	
cc-pVQZ(all)	1.7779	2.3583	2.1961	-168.492441	9427	
cc-pV5Z(all)	**1.7785**	**2.3567**	**2.1930**	**-168.528489**	**9355**	
cc-pCVDZ(all)	1.7896	2.3870	2.2327	-168.301688	10914	
cc-pCVTZ(all)	1.7803	2.3662	2.2021	-168.513099	9859	
cc-pCVQZ(all)	1.7795	2.3601	2.1965	-168.576113	9515	
cc-pCV5Z(all)	**1.7799**	**2.3590**	**2.1951**	**-168.595591**	**9392**	

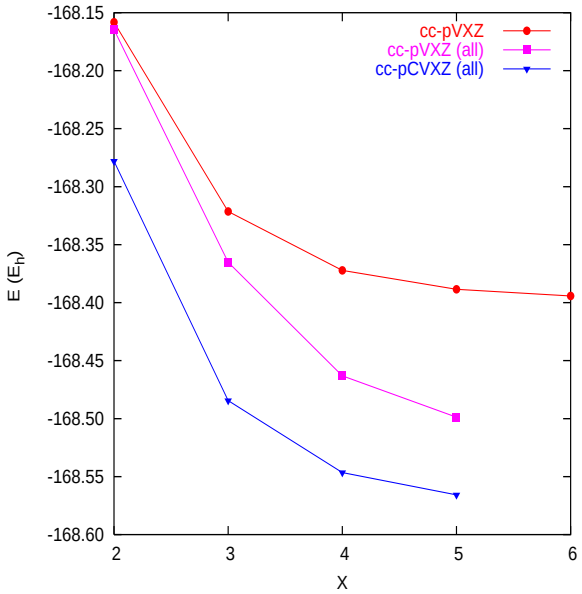

FIG. 2: Absolute CCSD(T) energy of optimized planar HCNO as a function of the cardinal number X of the cc-pVXZ, cc-pVXZ(all), and cc-pCVXZ(all) basis set families.

TABLE IV: Rotational constants (in cm^{-1}) of HCNO, HNCO, and HOCN, calculated using the structural parameters reported in Tables I, II, and III. Here, B$_{lin}$ stands for the rotational constant at the optimum linear arrangement.

HCNO	A$_e$	B$_e$	C$_e$	B$_{lin}$
cc-pV6Z	793	0.38250	0.38232	0.38214
cc-pCV5Z(all)	1410	0.38374	0.38364	0.38352
cc-pV5Z(all)	5315	0.38419	0.38417	0.38416
HNCO	A$_e$	B$_e$	C$_e$	B$_{lin}$
cc-pV6Z	27.659	0.36932	0.36445	0.36390
cc-pCV5Z(all)	28.138	0.37060	0.36578	0.36515
cc-pV5Z(all)	28.415	0.37128	0.36649	0.36588
HOCN	A$_e$	B$_e$	C$_e$	B$_{lin}$
cc-pV6Z	22.382	0.35256	0.34709	0.35108
cc-pCV5Z (all)	22.467	0.35393	0.34844	0.35235
cc-pV5Z(all)	22.520	0.35448	0.34899	0.35303

C$_e$, and B$_{lin}$ in Table IV agree within ca. 0.002 cm^{-1} (0.5 %). The scatter of rotational A$_e$ constants is 0.8 cm^{-1} (2.7 %) and 0.1 cm^{-1} (0.6%) for HNCO and HOCN, respectively. One may note that the two A$_e$ values obtained by correlating all electrons agree within 1 % for HNCO

TABLE V: Energies (in cm^{-1}) of optimized planar and linear HCNO and HOCN measured relative to the energy of the respective equilibrium HNCO configuration.

	planar HOCN	linear HOCN	planar HCNO	linear HCNO
cc-pVDZ	8131	19066	24208	24470
cc-pVTZ	8310	18231	24448	24490
cc-pVQZ	8489	18094	24558	24565
cc-pV5Z	8541	18030	24557	24558
cc-pV6Z	8567	18020	24554	24554
cc-pVDZ(all)	8173	19073	24210	24455
cc-pVTZ(all)	8491	18063	24217	24255
cc-pVQZ(all)	8612	18039	24471	24471
cc-pV5Z(all)	8647	18004	24523	24522
cc-pCVDZ(all)	8159	19073	24266	24500
cc-pCVTZ(all)	8335	18194	24471	24496
cc-pCVQZ(all)	8525	18040	24534	24536
cc-pCV5Z(all)	8577	17969	24516	24515

and 0.2 % for HOCN. Since optimized HCNO possesses two very nearly linear bond angles, the calculated A_e constant is rather large.

B. Relative energies

The barriers to linearity, E_{bar}, for HCNO, HNCO, and HOCN are given in the lower parts of Tables I, II, and III, respectively. For all three isomers, E_{bar} decreases as X increases, due to a somewhat faster lowering of the total energy at the linear arrangements upon increasing X. Planar HNCO and planar HOCN are 1907 and 9489 cm^{-1} more stable than their linear forms in the CCSD(T)/cc-pV5Z calculation. The inclusion of core correlation lowers the barrier to linearity by 149 cm^{-1} (ca. 8%) to 1758 cm^{-1} and by 134 cm^{-1} (ca. 1.4%) to 9355 cm^{-1}, respectively. The cc-pV5Z(all) and cc-pCV5Z(all) results agree within 3% for E_{bar}(HNCO) and 0.4% for E_{bar}(HNCO), Table II. This sensitivity of the barrier height to the level of correlation treatment is somewhat surprising if one considers the excellent consistency of equilibrium structures. A focal-point analysis by Császár at al.[40] carried out at the optimized CCSD(T)/cc-pVTZ(all) geometry of HNCO gave a barrier to linearity of 1864 cm^{-1}. The optimized CCSD(T)/cc-pVTZ(all) geometry [r_e(HN), r_e(NC), r_e(CO), $\angle(HNC)_e$, $\angle(NCO)_e$] for planar HNCO deviates, however, by [0.0014 a_0, 0.0073 a_0, 0.0082 a_0, -0.64°, -0.19°] from the corresponding CCSD(T)/cc-pV5Z(all) value, as seen in Table II. Niedenhoff at al.[24] derived a semirigid bender result of E_{bar}(HNCO)=1899 cm^{-1}. This result probably includes some effects due to vibrational averaging. Beyond the present treatment other effects on the HNCO barrier to linearity were found in the systematic study of relativistic corrections[41].

The relative energies of the CHNO isomers are summarized in Table V. Two of the entries in Table V can be compared with values obtained in a frozen-core focal-point study by Schuurman et al.[16], in which the empirical geometry of East et al.[18] was used for HNCO, the linear geometry of Koput et al.[14] for HCNO, and a CCSD(T)/cc-pVQZ optimized geometry for HOCN. Isomerization energies of 8621 cm^{-1} and 24717 cm^{-1} were reported for HOCN→HNCO and HCNO→HNCO, respectively, in the complete basis set (CBS) limit.[16] These results are 54 and 163 cm^{-1} larger than our values of 8567 cm^{-1} and 24554 cm^{-1}, listed for cc-pV6Z in Table V. This discrepancy is solely due to contributions of explicit triple substitutions, which amounts to 56 cm^{-1} and 130 cm^{-1} for CCSDT [see Table V of Ref.16]. The influence of core correlation on the two isomerization energies can be estimated from our Table V, which provides a value of 106 and 36 cm^{-1}, respectively, from the cc-pV5Z and cc-pV5Z(all) data.

C. Vibrational structures

The variation of the electronic (potential) energy along the minimum energy path (MEP) for the HCN bending angle of HCNO is displayed in Fig. 3. For the basis sets cc-pVXZ, cc-pVXZ(all), and cc-CVXZ(all) with X=2-4, the MEPs were calculated by relaxing the four coordinates r(HC), r(CN), r(NO), and ∠(CNO) for preselected values of ∠(HCN) in planar HCNO. In Fig. 3, one may note that the ordering of the MEPs for a given cardinal number X changes in going from $X = 2$ to $X = 4$. Whereas the CCSD(T)/cc-pVDZ(all) values lie between the other two sets of results for $X = 2$, the cc-pCVQZ(all) curve falls between cc-VQZ and cc-VQZ(all) for $X = 4$. The cc-pVQZ(all) values display the highest curvature in Fig. 3. The inclusion of core correlation effects leads to a visible stiffening of the bending profiles.

Figure 4 shows the CCSD(T)/cc-pVQZ(all) minimum

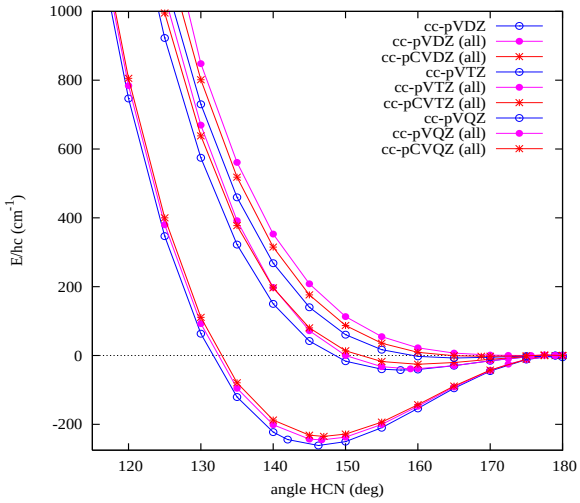

FIG. 3: Minimum energy path along the HCN angle of HCNO, calculated at the CCSD(T) level of theory for the cc-pVXZ and cc-pCVXZ basis sets using X=2-4. Both valence electron correlation and all electron correlation results are shown. For easier comparison, all profiles are drawn to a common scale.

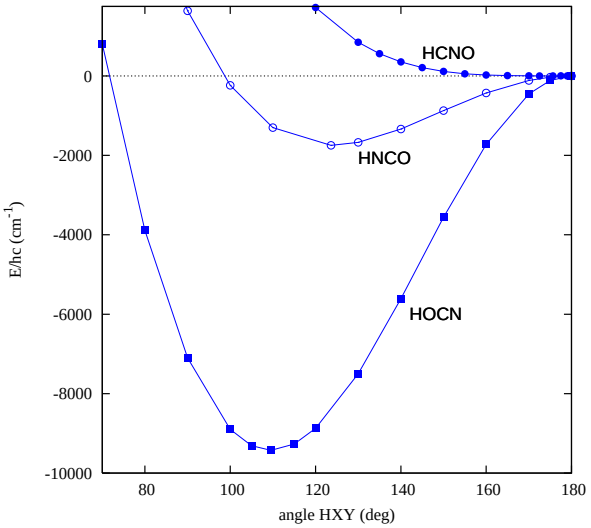

FIG. 4: Minimum energy paths of HCNO, HNCO, and HOCN from CCSD(T) calculations with the cc-pVQZ basis set and all electron correlation. Each of the curves shown is measured relative to the energy of the respective optimum linear configuration.

energy paths for planar HCNO, HNCO, and HOCN. Their common feature is a pronounced deviation from harmonic behaviour and a significant angular width. The variation of the optimum bond lengths r_{opt}(HX), r_{opt}(XY), and r_{opt}(YZ) along the MEPs of Fig. 4 is graphically presented in Fig. 5. For the MEP in the direction of the HCN bending angle of HCNO, the optimum triplet [r_{opt}(HC), r_{opt}(CN), r_{opt}(NO)] assumes the value of [2.032 a_0, 2.262 a_0, 2.243 a_0] for ∠(HCN)=120° and [2.000 a_0, 2.191 a_0, 2.269 a_0] for ∠(HCN)=180°, exhibiting changes of -0.032, -0.071, and +0.026 a_0, respectively. The decrease in r_{opt}(HX) and r_{opt}(XY), accompanied by an increase of r_{opt}(YZ), is also observed for HNCO and HOCN upon straightening of the HXY bending angle. These important changes of radial coordinates upon bending have strong effects on the bending dynamics through the reduced mass and typically lead to pronounced coupling between angular and radial vibrational modes in spite of widely differing frequency scales[43,44]. The variation of the CN bond length of HOCN is, however, rather weak, exhibiting changes of only 0.006 a_0 over the angular range explored in Fig. 5.

In Fig. 6, we compare the CCSD(T)/cc-pVQZ(all) MEP of HCNO with the MEPs of HCCH and HCCN. In addition to the MEP for the HCN angle, the MEP along the CNO angle is also displayed for HCNO. The potential energy surface of Strey and Mills[45] is used for HCCH only for the purpose of illustration. A MR-ACPF PES[27] is employed for HCCN. The small-amplitude CNO bending vibration in HCNO clearly resembles the stiff HCC bending mode of acetylene, a textbook example for linear molecules. The HCN bending mode, on the other side, is similar to the quasi-linear large amplitude HCC mode of HCCN, with the important difference that HCNO exhibits no barrier to linearity.

Coplanar atom arrangements of tetratomic molecules may have either *trans* or *cis* form. All the geometry optimizations starting at *cis* conformations of the CHNO isomers led to "hockey-stick" structures, arrangements with a strictly linear heavy-atom skeleton (we adopt here the terminology of East et al.[18]). There appear to be no local minima for *cis* arrangements. For HCNO, HNCO, and HOCN, the "hockey-stick" structures optimized at the cc-pVQZ(all) level are listed in Table VI. As seen there, the geometry optimization carried out by freezing the CNO subunit of HCNO to be linear led to the linear minimum of Table I. The optimum "hockey-stick" structures of HNCO and HOCN lie 339 and 31 cm^{-1} above their respective global minima, respectively. In the previous study on HCCN,[27] this structure was found 84 cm^{-1} above the minimum. It may be noted that the "hockey-stick" structures are relevant for the description of the torsional (out-of-plane bending) motion in tetratomic molecules.

Harmonic vibrational frequencies are collected in Table VII. The frequencies were evaluated numerically at the geometries optimized for the cc-pVXZ and cc-pVXZ(all) series with $X = 2 - 4$. For HCNO, which has a barrier to linearity of 7.44 and -0.03 cm^{-1} for the cc-pVQZ and cc-pVQZ(all) treatments, respectively, the force field analysis was carried out for both the planar and linear configurations of Table I. Two degenerate imaginary frequencies were found for linear HCNO and cc-pVQZ. For the two geometrically distinct, but energetically extremely close, HCNO configurations identified at the cc-pVQZ(all) level, harmonic vibrational frequencies

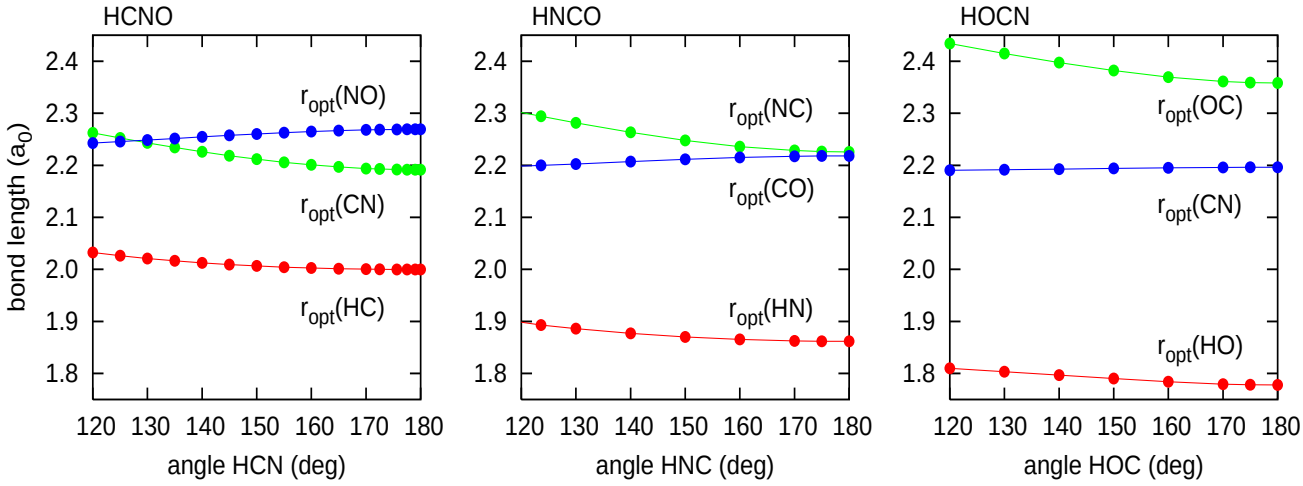

FIG. 5: Variation of the optimum bond lengths r_{opt}(HX), r_{opt}(XY), and r_{opt}(YZ) of HXYZ along the minimum energy path in the direction of the HXY angle from CCSD(T)/cc-pVQZ(all) calculations. The results are shown for HCNO (left), HNCO (center), and HOCN (right).

TABLE VI: Geometrical parameters for the "hockey-stick" structure of HCNO, HNCO, and HOCN at the CCSD(T)/cc-pVQZ(all) level. Bond lengths are given in a_0 and angles in degrees.

	HCNO		HNCO		HOCN
r(HC)$_e$	1.9997	r(HN)$_e$	1.8923	r(HO)$_e$	1.8181
r(CN)$_e$	2.1914	r(NC)$_e$	2.2895	r(OC)$_e$	2.4566
r(NO)$_e$	2.2692	r(CO)$_e$	2.2004	r(CN)$_e$	2.1896
$\angle$(HCN)$_e$	180.0	$\angle$(HNC)$_e$	123.34	$\angle$(HOC)$_e$	109.26
$\angle$(CNO)$_e$	180.0	$\angle$(NCO)$_e$	180.0	$\angle$(OCN)$_e$	180.0
E / E_h	-168.463134	E / E_h	-168.573087	E / E_h	-168.535252

are identical, with the exception of the quasi-linear HCN mode. A clear correlation can be seen between the ω_4(a') and ω_6(a") modes for planar HCNO on one side and the doubly degenerate CNO mode of linear HCNO on the other side. These harmonic estimates only give a first overview and will be replaced by a fully coupled anharmonic vibration-rotation treatment.

D. Computational perspectives

Since our main interest lies in the development of an accurate full-dimensional potential energy surface for HCNO, we address here several aspects of the *ab initio* treatment relevant from the computational point of view. An appropriate choice of one-electron basis functions and correlation method(s) is required to minimize the necessarily expensive electronic structure computations for several thousands of geometrical arrangements entering the construction of a full dimensional analytical representation.

The results presented in the preceeding sections have shown the importance of core correlation for the accurate description of all three CHNO isomers. The explicit inclusion of core electrons in correlated electronic structure calculations significantly increases the computational cost due to a larger one-electron basis set and a much larger number of many-electron configurations. For the basis sets of quadruple ζ quality, the number of primitive (contracted) Gaussian-type orbitals for the CHNO isomers is 286 (195) and 388 (282) for cc-pVQZ and cc-pCVQZ, respectively. The number of singly and doubly external configuration state functions (CSFs) in C_s symmetry increases from 552 481 and 1 199 875 for cc-pVQZ and cc-pCVQZ to 1 054 561 and 2 293 741 for cc-pVQZ(all) and cc-pCVQZ(all), respectively.

Single-point CCSD(T)/cc-pVQZ calculations in the frozen-core approximation take approximately 150, 500, and 1450 s for linear, planar, and general arrangements on a 2GHz clock rate dual-core computer and all-electron calculations with cc-pVQZ(all) approximately double the execution times. Replacement of the cc-pVQZ(all) treatment by a cc-pCVQZ(all) treatment increases the timing for a single-point all-electron CCSD(T) calculation by a factor of ca. 4 to 1400, 4000, and 12 000 s for a linear,

TABLE VII: Harmonic wavenumbers (in cm^{-1}) of HCNO, HNCO, and HOCN, computed at the optimized geometries reported in Tables I, II, and III. For ease of visualization, we abbreviate with VXZ the basis set cc-pVXZ. The symmetry labels of the C_s point group are used here.

HCNO	VDZ	VTZ	VQZ	VQZ linear	VDZ(all)	VTZ(all)	VQZ(all)	VQZ(all) linear	normal mode
ω_1(a')	3426	3467	3479	3493	3434	3486	3504	3505	C-H stretch
ω_2(a')	2217	2250	2267	2280	2223	2273	2295	2296	C-N-O as.stretch
ω_3(a')	1288	1274	1273	1269	1290	1287	1279	1279	C-N-O s.stretch
ω_4(a')	542	553	554	555,555	544	566	565	565,565	C-N-O bend
ω_5(a')	459	301	194	128i,128i	454	299	85	33,33	H-C-N bend
ω_6(a")	545	554	554		547	567	565		torsion
HNCO	VDZ	VTZ	VQZ		VDZ(all)	VTZ(all)	VQZ(all)		normal mode
ω_1(a')	3660	3688	3693		3667	3713	3711		N-H stretch
ω_2(a')	2299	2307	2307		2304	2329	2324		N-C-O as.stretch
ω_3(a')	1292	1304	1311		1295	1319	1321		N-C-O s.stretch
ω_4(a')	855	825	818		854	809	805		H-N-C bend
ω_5(a')	547	562	567		549	566	568		N-C-O bend
ω_6(a")	609	625	631		610	633	634		torsion
HOCN	VDZ	VTZ	VQZ		VDZ(all)	VTZ(all)	VQZ(all)		normal mode
ω_1(a')	3793	3805	3809		3796	3823	3817		H-O stretch
ω_2(a')	2305	2320	2325		2309	2341	2338		C-N stretch
ω_3(a')	1288	1275	1270		1288	1269	1273		H-O-C bend
ω_4(a')	1063	1074	1079		1066	1086	1086		C-O stretch
ω_5(a')	407	427	432		409	431	435		O-C-N bend
ω_6(a")	462	484	489		464	497	494		torsion

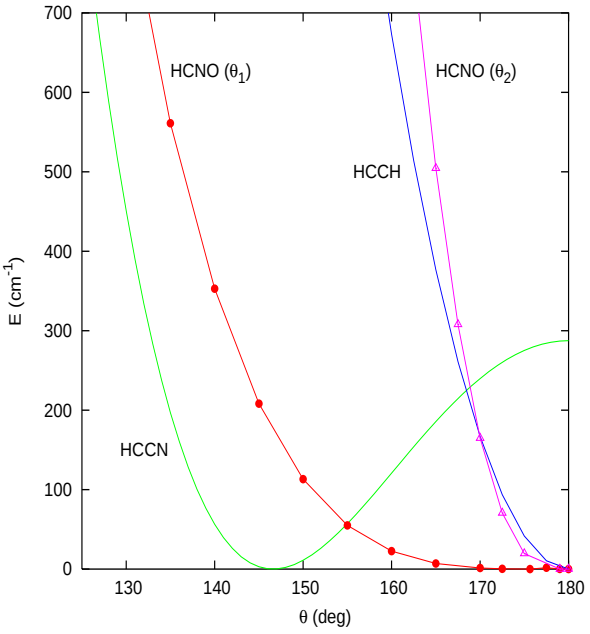

FIG. 6: Minimum energy paths along the bending angle for the HCNO, HCCN, and HCCH molecules. The angle HXY denotes the HCN angle θ_1 of HCNO and the HCC angle of HCCN and HCCH, respectively. An additional profile is shown for the CNO angle θ_2 in HCNO. For more details, see the text.

planar, and spatial geometry, respectively. CCSD(T)/cc-pV5Z computations in the frozen-core approximation took approximately 1350, 3500, and 11 000 s, largely excluding a basis set of quintuple ζ quality for the scanning of the PES in the computationally even more expensive all-electron approach.

Since the cc-pCVXZ basis set family is specifically designed for core-core and core-valence correlation, we also tested the performance of cc-pCVQZ in combination with the frozen-core approximation. These calculations yielded an equilibrium structure of [2.0060 a_0, 2.2009 a_0, 2.2721 a_0, 164.91°, 176.53°] at an energy of -168.375308 E_h for planar HCNO and of [2.0042 a_0, 2.1956 a_0, 2.2748 a_0, 180.0°, 180.0°] at an energy of -168.375271 E_h for linear HCNO, yielding a barrier to linearity of 6.70 cm^{-1}. Due to the striking similarity of these results with the cc-pVQZ values from Table I, we have not pursued further the cc-pCVXZ calculations with valence correlations only.

Two basis sets emerge from our current study as candidates for the development of the full PES, namely cc-pVQZ(all) and cc-pCVQZ(all). Inspection of Tables I, II, and III, together with Figs. 1 and 3, clearly shows a more balanced performance for cc-pCVXZ(all), accompanied with a monotonic convergence behaviour for the quantities studied here. In view of much higher CPU requirements of the cc-pCVQZ calculation, we however consider developing a PES based only on the cc-pVQZ(all) points. This cc-pVQZ(all) PES may subsequently be im-

TABLE VIII: RHF barrier to linearity and correlation energy contribution to the CCSD(T) barrier to linearity obtained for HCNO at the optimized cc-pV6Z, cc-pV5Z(all), and cc-pCV5Z(all) geometries (first three rows) and the optimized frozen core cc-pV5Z geometry denoted here by *geo*5 (last five rows). The latter series of calculations, cc-pVXZ(*geo*5), is carried out at the geometry *geo*5 with the cc-pVXZ basis set for $X = 2 - 6$. The optimized geometries are taken from Table I. All quantities are given in cm^{-1}. For more details, see the text.

	RHF	Correlation contribution
cc-pV6Z	-123.6	123.3
cc-pV5Z(all)	-20.3	19.9
cc-pCV5Z(all)	-70.0	69.1
cc-pVDZ(*geo*5)	-163.5	219.7
cc-pVTZ(*geo*5)	-182.5	201.7
cc-pVQZ(*geo*5)	-185.7	191.5
cc-pV5Z(*geo*5)	-186.7	187.6
cc-pV6Z(*geo*5)	-186.7	185.4

proved through a fractional inclusion of higher quality cc-pCVQZ(all) points or alternatively adjusted to reproduce selected experimental data, as previously done in the study on HCCN[27].

IV. CONCLUSION

Rovibrational calculations with exact hamiltonians require reliable potential energy surfaces covering large regions of configuration space. Checking the convergence of available electronic structure methods is a mandatory initial step for the identification of a strategy which combines sufficient accuracy with acceptable computational cost. Our systematic investigation of the impact of basis set size and level of correlation treatment have confirmed the previously observed difficulties to arrive at a converged equilibrium geometry for the HCNO molecule whose rovibrational spectrum is particularly rich and complicated. We believe, however, to have shown beyond reasonable doubt that HCNO is indeed linear at electronic equilibrium. The inclusion of core correlation and high angular momentum basis functions proved to be essential to arrive at this result. Similar, but less pronounced, effects of core correlation were found for the isomers HNCO and HOCN, the most notable being a surprising sensitivity of the barrier to linearity. It remains an open question if the difficulty of converging to the linear arrangement reflects merely the intrinsic physics of the HCNO molecule or some subtle symmetry breaking effects in the electronic structure methodology.

To demonstrate and rationalize the difficulties encountered in the present study, we finally summarize in Table VIII the RHF barriers to linearity for HCNO, obtained at several selected CCSD(T) geometries. The barrier E_{bar} to linearity is calculated as common, $E_{bar}=E_{lin}-E_{min}$, such that a negative E_{bar} corresponds to a situation of a more stable linear configuration (*lin*). In the correlation treatment, the zero-order RHF solution is improved by adding the correlation energy contribution. The CCSD(T) correlation contribution to E_{bar} increases the barrier to linearity of HCNO, i.e. it favours its non-linear coplanar arrangement, as seen in Table VIII. The final CCSD(T) result for E_{bar} appears to be the result of a very subtle interplay between the two energy parts, the dominant RHF energy and the small correlation energy contribution, whose effects on E_{bar} are varying in the opposite sense.

The analysis of minimum energy paths on the HCNO surface indicates an extreme flatness of the surface upon bending and the presence of strong angular-radial coupling. The latter effect can easily lead to the appearance of an adiabatic barrier at the linear arrangement, such that the molecule effectively behaves as slightly non-linear, as previously proposed by Bunker et al.[10]. A distinct advantage of progressive subspace diagonalisation and truncation discrete variable approaches[46,47] over alternative techniques[48] is the possibility to visualise the dynamics of large amplitude motions through the construction of effective adiabatic potentials for low frequency modes at given excitations of other vibrational modes. The application of this type of analysis to the potential energy surface and rovibrational dynamics of the quasi-linear molecule HCCN indicated very strong variations of the effective barrier to linearity upon excitation of stretching modes.[27] The structure of the minimum energy paths on the HCNO surface lets us expect similar coupling effects between high and low frequency modes.

Acknowledgments

Both authors have enjoyed the privilege of working in the theoretical chemistry group of S. D. Peyerimhoff at the University of Bonn in their very early career, albeit without meeting each other there. The friendly and exciting atmosphere and the possibility of contributing to advanced research projects as an undergraduate student left an unforgettable mark on ML and laid the foundation for a successful return into theory after fruitful years spent with experimental work.

* Corresponding author; Electronic address: mladenov@univ-mlv.fr

† Electronic address: lewerenz@univ-mlv.fr

[1] W. R. Thorson and I. Nakagawa, J. Chem. Phys. 33 (1960)

994.
[2] B. P. Winnewisser, In K. Narahari Rao, editor, *Molecular Spectroscopy: Modern Research* volume 3. Academic Press Orlando 1985.
[3] M. Winnewisser, B. P. Winnewisser, I. R. Medvedev, F. C. De Lucia, S. C. Ross and L. M. Bates, J. Mol. Struct. 798 (2006) 1.
[4] B. P. Winnewisser, M. Winnewisser and F. Winther, J. Mol. Spectrosc. 51 (1974) 65.
[5] E. L. Ferretti and K. Narahari Rao, J. Mol. Spectrosc. 51 (1974) 97.
[6] K. Yamada, B. P. Winnewisser and M. Winnewisser, J. Mol. Spectrosc. 56 (1975) 449.
[7] B. P. Winnewisser and P. Jensen, J. Mol. Spectrosc. 101 (1983) 408.
[8] S. Albert, M. Winnewisser and B. P. Winnewisser, Ber. Bunsenges. 100 (1996) 1876.
[9] S. Albert, K. K. Albert, M. Winnewisser and B. P. Winnewisser, J. Mol. Spectrosc. 599 (2001) 347.
[10] P. R. Bunker, B. M. Landsberg and B. P. Winnewisser, J. Mol. Spectrosc. 74 (1979) 9.
[11] M. T. Nguyen, K. Pierloot and L. G. Vanquickenborne, Mol. Phys. 78 (1993) 319.
[12] A. P. Rendell, T. J. Lee and R. Lindh, Chem. Phys. Lett. 194 (1992) 84.
[13] N. Pinnavaia, M. J. Bramley, M.-D. Su, W. H. Green and N. C. Handy, Mol. Phys. 78 (1993) 319.
[14] J. Koput, B. P. Winnewisser and M. Winnewisser, Chem. Phys. Lett. 255 (1996) 357.
[15] A. M. Mebel, A. Luna, M. C. Lin and K. Morokuma, J. Chem. Phys. 105 (1996) 6439.
[16] M. S. Schuurman, S. R. Muir, W. D. Allen and H. F. Schaefer III, J. Chem. Phys. 120 (2004) 11586.
[17] D. C. McKean, J. L. Duncan and L. Batt, Spectrochim. Acta 29A (1973) 1037.
[18] A. L. L. East, C. S Johnson and W. D. Allen, J. Chem. Phys. 98 (1993) 1299.
[19] D. Poppinger, L. Radom and J. A. Pople, J. Am. Chem. Soc. 99 (1977) 7806.
[20] J. H. Teles, G. Maier, B. A. Hess, Jr., L. J. Schaad, M. Winnewisser and B. P. Winnewisser, Chem. Ber. 122 (1989) 753.
[21] J.-A. Miller and C. T. Bowman, Int. J. Chem. Kin. 23 (1991) 289.
[22] R. Homma and J.-Y. Chen, J. Mol. Spectrosc. 123 (2001) 303.
[23] J.-Y. Park and D. E. Woon, ApJ 601 (2004) L63.
[24] M. Niedenhoff, K. M. T. Yamada, M. Winnewisser and S. C. Ross, J. Mol. Struct. 352 (1995) 423.
[25] M. E. Jacox and D. E. Milligan, J. Chem. Phys. 40 (1964) 2457.
[26] R. N. Dixon, Trans. Far. Soc 60 (1964) 1363.
[27] M. Mladenović, P. Botschwina and C. Puzzarini, J. Phys. Chem. 110 (2006) 5520.
[28] M. Mladenović, J. Chem. Phys. 112 (2000) 1070.
[29] T. H. Dunning, Jr., J. Chem. Phys. 90 (1989) 1007.
[30] D. E. Woon and T. H. Dunning, Jr., J. Chem. Phys. 103 (1995) 4572.
[31] MOLPRO, version 2006.1, a package of ab initio programs, H.-J. Werner, P. J. Knowles, R. Lindh, F. R. Manby, M. Schütz, P. Celani, T. Korona, G. Rauhut, R. D. Amos, A. Bernhardsson, A. Berning, D. L. Cooper, M. J. O. Deegan, A. J. Dobbyn, F. Eckert, C. Hampel and G. Hetzer, A. W. Lloyd, S. J. McNicholas, W. Meyer and M. E. Mura, A. Nicklass, P. Palmieri, R. Pitzer, U. Schumann, H. Stoll, A. J. Stone, R. Tarroni and T. Thorsteinsson , see http://www.molpro.net.
[32] C. Hampel, K. A. Peterson and H.-J. Werner, Chem. Phys. Lett. 190 (1992) 1, and references therein.
[33] M. J. O. Deegan and P. J. Knowles, Chem. Phys. Lett. 227 (1994) 321.
[34] F. Eckert, P. Pulay and H.-J. Werner, Theor. Chem. Acc. 100 (1998) 21.
[35] G. Rauhut, A. El Azhary, F. Eckert, U. Schumann and H.-J. Werner, Spectrochim. Acta, Part A 55 (1999) 651.
[36] M. Rosenstock, P. Rosmus, E. A. Reinsch, O. Treutler, S. Carter and N. C. Handy, Mol. Phys. 93 (1998) 853.
[37] T. J. Lee and P. R. Taylor, Int. J. Quant. Chem. Symp. 23 (1989) 199.
[38] F. Jensen, Introduction to Computational Chemistry, (Wiley, New York, 2007), 2nd ed.
[39] J. Demaison, L. Margulès and J. E. Boggs, Chem. Phys. 260 (2000) 65.
[40] A. G. Császár, W. D. Allen and H. F. Schaefer III, J. Chem. Phys. 108 (1998) 9751.
[41] G. Tarczay, A. G. Császár, W. Klopper and H. M. Quiney, Mol. Phys. 99 (2001) 1769.
[42] I. Mills, T. Cvitaš, K. Homann, N. Kallay and K. Kuchitsu, Quantities, Units and Symbols in Physical Chemistry, Second Edition, (Blackwell Scientific Publications, Oxford, 1993).
[43] I. M. Mills, J. Phys. Chem. 88 (1984) 532.
[44] M. Mladenović and M. Lewerenz, Chem. Phys. Lett. 321 (2000) 135.
[45] G. Strey and I. M. Mills, J. Mol. Spectrosc. 59 (1976) 103.
[46] Z. Bačić and J. C. Light, Annu. Rev. Phys. Chem. 40 (1989) 469.
[47] M. Mladenović, Spectrochim. Acta, Part A 58 (2002) 795.
[48] J. Light and T. Carrington, Jr., Adv. Chem. Phys. 114 (2000) 263.